



## Abstract

Black carbon (BC) and dust deposited on snow and glacier surfaces can reduce the surface albedo, accelerate snow and ice melt, and trigger albedo feedback. Assessing BC concentrations in snow and ice in the Himalaya is of interest because this region borders large BC sources, and seasonal snow and glacier ice in this region are an important source of water resources. Snow and ice samples were collected from crevasse profiles and snowpits at elevations between 5400 and 6400 m a.s.l. from Mera glacier located in the Solu-Khumbu region of Nepal on the southern slope of the Himalaya during spring and fall 2009. The samples were measured for Fe concentrations (used as a dust proxy) via ICP-MS, total impurity content gravimetrically, and BC concentrations using a Single Particle Soot Photometer (SP2). Measured BC concentrations underestimate actual BC concentrations due to changes to the sample during storage, and loss of BC particles in the ultrasonic nebulizer. BC and Fe concentrations peak during the winter–spring, and are substantially higher at elevations  $< 6000$  m due to post-depositional processes including melt and sublimation and greater loading in the lower troposphere. Because the largest areal extent of snow and ice resides at elevations  $< 6000$  m, the higher BC and dust concentrations at these elevations can reduce the snow and glacier albedo over large areas, accelerating melt, affecting glacier mass-balance and water resources, and contributing to a positive climate forcing. Radiative transfer modeling constrained by measurements indicates that BC concentrations in the winter–spring snow/ice horizons are sufficient to reduce albedo by 6–10 % relative to clean snow, corresponding to instantaneous radiative forcings of  $75$ – $120$   $\text{W m}^{-2}$ . The other bulk impurity concentrations, when treated separately as dust, reduce albedo by 40–42 % relative to clean snow and give instantaneous radiative forcings of 490 to  $520$   $\text{W m}^{-2}$ . Adding the BC absorption to the other impurities results in additional radiative forcings of 3–10  $\text{W m}^{-2}$ . While BC contributes to accelerated snow and ice melt, the impact of BC is diminished in the presence of other light absorbing impurities. However, the time span of the BC exposure at the snow surface in the dry winter–spring

## Variations of black carbon and dust in snow and ice

S. Kaspari et al.

[Title Page](#)

[Abstract](#)

[Introduction](#)

[Conclusions](#)

[References](#)

[Tables](#)

[Figures](#)

[◀](#)

[▶](#)

[◀](#)

[▶](#)

[Back](#)

[Close](#)

[Full Screen / Esc](#)

[Printer-friendly Version](#)

[Interactive Discussion](#)



season is likely a persistent forcing before impurity convergence, but is not addressed by these single measurements. Further observational studies are needed to assess the contribution of BC relative to other absorbing impurities to albedo reductions and snow and ice melt.

## 5 1 Introduction

Recent research has focused on assessing black carbon (BC, the strongest absorbing component of soot) concentrations in snow and ice. BC is produced by the incomplete combustion of biomass, coal and diesel fuels. In the atmosphere, BC absorbs light and causes atmospheric heating, whereas BC deposited on snow and ice can reduce the 10 surface albedo, accelerate snow and ice melt, and trigger albedo feedback (Flanner et al., 2009; Hansen and Nazarenko, 2004; Ramanathan and Carmichael, 2008). BC is estimated to be second only to  $\text{CO}_2$  in its contribution to climate forcing (Ramanathan and Carmichael, 2008; Bond et al., 2013), and the effect of BC on snow albedo further contributes to climate warming (Hansen and Nazarenko, 2004). However, the degree 15 to which BC contributes to climate warming and change in the hydrologic cycle remains uncertain.

Assessing BC concentrations in the Himalaya and Tibetan Plateau is of particular interest because this region borders some of the largest sources of BC globally (Bond et al., 2007). Regional sources of BC include biomass burning (forest and grassland 20 fires, burning of agricultural and crop waste), residential cooking and heating, transportation, power generation, and industry (Bond et al., 2004; Venkataraman et al., 2005, 2006). The largest climate forcing from BC in snow is estimated to occur over the Himalaya and Tibetan Plateau (Ramanathan and Carmichael, 2008; Flanner et al., 2007, 2009), and there are concerns that BC is contributing to glacier retreat in this 25 region via atmospheric heating and albedo reduction due to BC deposition on glacier surfaces (Ramanathan and Carmichael, 2008). Glacier retreat in this region has serious consequences as snow and runoff from Himalayan glaciers are the source of major

<a href="#">Title Page</a>	
<a href="#">Abstract</a>	<a href="#">Introduction</a>
<a href="#">Conclusions</a>	<a href="#">References</a>
<a href="#">Tables</a>	<a href="#">Figures</a>
<a href="#">◀</a>	<a href="#">▶</a>
<a href="#">◀</a>	<a href="#">▶</a>
<a href="#">Back</a>	<a href="#">Close</a>
<a href="#">Full Screen / Esc</a>	
<a href="#">Printer-friendly Version</a>	
<a href="#">Interactive Discussion</a>	



**Variations of black carbon and dust in snow and ice**

S. Kaspari et al.

[Title Page](#)[Abstract](#)[Introduction](#)[Conclusions](#)[References](#)[Tables](#)[Figures](#)[|◀](#)[▶|](#)[◀](#)[▶|](#)[Back](#)[Close](#)[Full Screen / Esc](#)[Printer-friendly Version](#)[Interactive Discussion](#)

rivers in Asia and the availability of water resources has profound effects on agriculture and human health (Barnett et al., 2005; Immerzeel et al., 2010).

Prior research has begun to characterize BC concentrations in snow and ice in this region both spatially and temporally. Ming et al. (2009) analyzed snowpits for BC from 5 glaciers in Western China and reported that BC concentrations are highest on the periphery of the Tibetan Plateau and at lower elevations, likely due to the closer vicinity to sources, and melting, which concentrates the BC load. Historical records of BC concentrations in snow and ice have been produced from ice cores retrieved from mountain glaciers, with most studies reconstructing BC concentrations since the 1950s. 10 These studies suggest that BC concentrations on the Tibetan Plateau were highest during the 1950s–1960s, during which Tibetan glaciers retreated, whereas cores from the Himalaya indicate elevated BC concentrations in recent decades (Liu et al., 2008; Ming et al., 2008; Xu et al., 2009). A Mt. Everest ice core spanning 1860–2000 provided the first Asian ice core record of BC concentrations since pre-industrial times, 15 and documented a threefold increase in BC concentrations from 1975–2000 relative to 1860–1975 (Kaspari et al., 2011). The differences in BC temporal trends between sites is attributed to source differences, with the Tibetan Plateau sites thought to be dominated by European BC sources, whereas modeling studies and comparisons of ice core records with historical BC emission inventories suggest that the dominant 20 sources of BC deposited in the Himalaya are from South Asia, with lesser contributions from the Middle East (Kopacz et al., 2011; Kaspari et al., 2011; Bond et al., 2007; Xu et al., 2009).

Previous BC observational work has focused on BC concentrations in snow and ice on the northern slope of the Himalaya, despite the proximity of the south slope 25 of the Himalaya to major BC sources (Fig. 1). Herein we present BC concentrations from snow and ice from the Solu-Khumbu region of Nepal, providing the first snow and ice observational data from the south side of the Himalaya. We investigate how BC concentrations vary seasonally and with elevation due to differences in BC deposition and post-depositional processes, and we estimate the associated changes in albedo

and radiative forcings by BC in snow. While recent research has largely focused on BC, dust and other light absorbing impurities also reduce snow albedo and can be present in snow in much higher concentrations than BC (e.g., Kaspari et al., 2011; Painter et al., 2007; Takeuchi et al., 2002). Furthermore, there is evidence that dust deposition in the 5 Himalaya may be increasing due to anthropogenic activities and increased aridity, and that dust may dominate solar absorption (e.g., Thompson et al., 2000; Kaspari et al., 2009; Gautam et al., 2013; Ming et al., 2012). Thus, we also estimate changes in albedo and radiative forcings from dust and dust mixed with BC.

## 2 Site description and methods

### 10 2.1 Site

To characterize BC and dust concentrations in snow and ice, snow/ice samples were collected during spring and fall 2009 at elevations between 5400 and 6400 m a.s.l. from Mera glacier ( $27^{\circ}43' N$ ,  $86^{\circ}53' E$ ), Solu-Khumbu region of Nepal on the southern slope of the Himalaya (Fig. 2). All samples were collected in pre-cleaned 50 mL polypropylene vials. In late April 2009, crevasse profiles were sampled in order to sample multiple 15 years of firn. The outer 10 cm of the crevasse wall was removed using a mountain axe, and the crevasse wall was continuously sampled in 5–10 cm increments directly into vials. The upper 3 m of a crevasse was sampled at 5400 m a.s.l. near Mera La, and the upper 2 m of a crevasse was sampled at 5800 m a.s.l. below Mera High Camp. 20 At the col below Mera Peak (6400 m a.s.l.) a 54 cm snowpit was continuously sampled in 3 cm increments. In addition to the snow/firn collected from Mera glacier, nine fresh snow samples were collected by personnel at the Nepal Climate Observatory-Pyramid (NCO-P) in the Khumbu Valley, Nepal ( $27^{\circ}56' N$ ,  $86^{\circ}49' E$ , 5079 m a.s.l.) during February–May 2009. These samples were kept frozen until transport from NCO-P. 25 To access Mera glacier requires several days on foot. Due to the remoteness of the site, samples were not kept frozen during transport from the field to the laboratory.

<a href="#">Title Page</a>	
<a href="#">Abstract</a>	<a href="#">Introduction</a>
<a href="#">Conclusions</a>	<a href="#">References</a>
<a href="#">Tables</a>	<a href="#">Figures</a>
<a href="#">◀</a>	<a href="#">▶</a>
<a href="#">◀</a>	<a href="#">▶</a>
<a href="#">Back</a>	<a href="#">Close</a>
<a href="#">Full Screen / Esc</a>	
<a href="#">Printer-friendly Version</a>	
<a href="#">Interactive Discussion</a>	



Thus, samples were kept stored at ambient temperature away from light until analyzed for BC and dust at the Paul Scherrer Institut in May 2009. Additionally, during early November 2009 a 30 cm snowpit was sampled at 5 cm resolution from Mera La, a 1.2 m snowpit was sampled at 3–4 cm resolution below Mera High Camp, and a 1.7 m snowpit was sampled at 3.7 cm resolution at the col below Mera peak. These samples were stored at ambient temperature until analyzed in October 2010 at Central Washington University. Due to the longer time period between collection and chemical analysis of the samples collected during the fall of 2009, these samples are only discussed briefly.

## 2.2 Methods

All samples were acidified with nitric acid to  $0.5 \text{ mol L}^{-1}$  for consistency with the methods described in Kaspari et al. (2011). Iron (Fe) concentrations were determined by inductively coupled plasma mass spectrometry (ICP-MS) and used as a dust proxy because iron oxides dominate light absorption by mineral dust. The impurity load in selected highly concentrated samples was determined gravimetrically after drying the samples at  $80^\circ\text{C}$ , and herein the dry mass is treated as dust. For BC, the samples were sonicated for 15 min just prior to analysis. During BC analyses the samples were mixed using a magnetic stirrer, nebulized using a Cetac U-5000AT+ ultrasonic nebulizer, and the resultant aerosol was introduced to the sample inlet of a Single Particle Soot Photometer (SP2, Droplet Measurement Technologies). Samples with measured BC concentrations exceeding  $10 \mu\text{g L}^{-1}$  were diluted with MQ water to less than  $10 \mu\text{g L}^{-1}$ .

The SP2 uses laser-induced incandescence to measure the BC mass in individual particles (between 80–500 nm diameter in this study) quantitatively and independent of particle morphology and coatings with light scattering material (Slowik et al., 2007; Schwarz et al., 2006; Stephens et al., 2003). The SP2 detects the mass concentration of refractory BC (sometimes referred to as rBC (Petzold et al., 2013); the term BC is used here for simplicity), while other absorbing aerosol components such as brownish carbon or mineral dust generally are not detected by the SP2. Recent work indicates that the presence of dust can produce visible light signals in the SP2, which causes

<a href="#">Title Page</a>	
<a href="#">Abstract</a>	<a href="#">Introduction</a>
<a href="#">Conclusions</a>	<a href="#">References</a>
<a href="#">Tables</a>	<a href="#">Figures</a>
<a href="#">◀</a>	<a href="#">▶</a>
<a href="#">◀</a>	<a href="#">▶</a>
<a href="#">Back</a>	<a href="#">Close</a>
<a href="#">Full Screen / Esc</a>	
<a href="#">Printer-friendly Version</a>	
<a href="#">Interactive Discussion</a>	



a small positive offset ( $15 \mu\text{g L}^{-1}$  BC offset for samples with very high ( $50\,000 \mu\text{g L}^{-1}$ ) dust concentrations) (Schwarz et al., 2012). In the context of this study, this offset is negligible due to the high BC concentrations reported herein, and other analytical uncertainties described below. Further details on the SP2 calibration and configuration are provided by Wendl et al. (2013) and in the auxiliary materials of Kaspari et al. (2011).

Monitoring of liquid sample flow rate pumped into the nebulizer, fraction of liquid sample nebulized, and nebulizer and SP2 airflow rates allows BC mass concentrations in the liquid sample to be determined. Schwarz et al. (2012) report that the SP2 combined with a Collison-type nebulizer can be used to measure BC mass concentration in snow with an estimated 60 % uncertainty (due to uncertainty in calibration results and size dependent nebulization efficiency). The BC concentrations reported herein underestimate actual concentrations, and have an uncertainty higher than 60 % due to:

1. Loss of BC particles in the Cetac U-5000AT+ ultrasonic nebulizer. Schwarz et al. (2012) tested nebulization efficiency based on particle size using polystyrene latex spheres ranging in size between 220 and 1537 nm, and reported that the Cetac nebulization efficiency was size dependent. The nebulization efficiency was 20 % or less for particles greater than 700 nm relative to particles in the 200–500 nm size range. Subsequent research at CWU confirmed the results of Schwarz for the Cetac, while Wendl et al. (2013) found that for the Cetac nebulization efficiency was greatest in the 300–400 nm size range, with decreased efficiency for smaller and larger particle sizes. Additionally, Schwarz et al. (2013) report larger mass size distributions of BC in snow than BC in the atmosphere, with the mass of BC cores larger than 600 nm accounting for 17 % or more of the BC mass based on snow samples in Colorado. Thus, a non-trivial mass of BC is not nebulized by the Cetac nebulizer, and thus not measured by the SP2. We correct for the mass of BC not nebulized based on gravimetric Aquadag standard solutions. This standard correction does not fully address the size dependent

**Variations of black carbon and dust in snow and ice**

S. Kaspari et al.

[Title Page](#)[Abstract](#)[Introduction](#)[Conclusions](#)[References](#)[Tables](#)[Figures](#)[|◀](#)[▶|](#)[◀](#)[▶](#)[Back](#)[Close](#)[Full Screen / Esc](#)[Printer-friendly Version](#)[Interactive Discussion](#)

# Variations of black carbon and dust in snow and ice

S. Kaspari et al.

## Title Page

## Abstract

## Introduction

## Conclusions

## References

## Tables

## Figures

Page 10

100% of the energy consumed in the United States is derived from fossil fuels.

1

1

Back

Close

Full Screen / Esc

[Printer-friendly Version](#)

## Interactive Discussion



nebulization nor likely differences in the mass-size distributions of Aquadag and the snow samples. We also note that prior studies using the SP2 to measure BC concentrations in liquid samples have used other BC materials as a calibration standard, with other standards resulting in a higher corrected BC concentration than Aquadag (Wendl et al., 2013).

2. Apparent BC losses due to changes to the sample during storage. Repeated measurements on aqueous samples stored at ambient temperature demonstrate a reduction in measured BC concentrations over time (Wendl et al., 2013). Re-measuring Aquadag standards and environmental samples stored at room temperature in polypropylene vials over an 18 day period indicated that BC losses are dependent on sample concentration. Aquadag standards that measured 7, 5 and 2  $\mu\text{g L}^{-1}$  BC directly after the standards were created decreased to 4, 1.8 and 0.3  $\mu\text{g L}^{-1}$  BC, indicating that measured concentrations after 18 days were 57, 36 and 15 % of the initially measured concentrations, respectively. An environmental snow sample that initially was measured as having a concentration of 2.4  $\mu\text{g L}^{-1}$  BC decreased to 0.6  $\mu\text{g L}^{-1}$  after 18 days, or 25 % of the initially measured concentration (Wendl et al., 2013). These results suggest that apparent BC losses are proportionally greater in low concentration samples relative to higher concentration samples. The samples from Mera glacier were analyzed three weeks after sample collection, so the above-mentioned BC losses may be referred to in order to estimate apparent BC losses in the Mera samples. However, complications in extrapolating the above results to the Mera samples include (1) BC concentrations in some of the Mera samples are one to two magnitudes greater than the prepared standards. BC losses in highly concentrated samples are likely proportionally lower than low concentration samples, as indicated by the above results, and (2) the Mera samples have high dust concentrations, and it is not known how the chemical composition of the sample affects apparent BC losses. Possible causes of the BC losses during storage include BC particles agglomerating above the size range in which particles are efficiently nebulized and outside of

the detection range of the SP2, and/or BC adhering to the vial walls. Subsequent research has shown that acidification of samples stored in polypropylene can aid in at least partial recovery of BC losses that occur in the sample vial (Wendl et al., 2013). However, in general we advise against acidification because acidification can cause a shift towards smaller BC particles (Schwarz et al., 2012). To avoid particle losses, samples should be kept frozen from the time of collection until just prior to being measured with the SP2. As mentioned above, field logistics during this reconnaissance campaign did not make this possible in the current study.

These factors lead to uncertainties in the actual BC concentrations. Herein we report the BC concentrations as *measured* BC ( $M_{BC}$ ), which have been corrected for the nebulizer efficiency based on the Aquadag standard solutions. The  $M_{BC}$  concentrations do not account for BC particles larger than those detected by our Cetac-SP2 system, nor BC particle losses that occurred during storage. Thus, the data reported herein represent lower limit values, and we predominantly focus our interpretation on relative differences in BC rather than on absolute concentrations. That the BC losses are not constant across all samples does not prevent interpretation since we focus on periods of peak signal, and  $M_{BC}$  concentrations span three orders of magnitude. Despite the uncertainties in the data, the results reported herein yield information that furthers our understanding of seasonal and spatial variations in BC in snow and ice in the Himalaya.

## 20 3 Results and discussion

### 3.1 Seasonal variations of BC

Within the two crevasse profiles, layers of impurities were observed in the firn, interspersed with thicker low impurity firn layers (Fig. 3). The impurity layers are particularly distinct at lower elevation Mera La. Peak concentrations of  $MBC$  and Fe coincide with the visible impurity layers.

Previous research in the region has documented strong seasonality in BC and dust concentrations, with peak concentrations during the winter–spring, and lower concentrations during the summer monsoon season. This seasonality has been observed in ice cores and snowpits (Kaspari et al., 2011; Cong et al., 2009), and atmospheric measurements from NCO-P (Marinoni et al., 2010; Bonasoni et al., 2010). Factors controlling the BC and dust seasonality include variations in emissions, atmospheric transport, and precipitation (Kaspari et al., 2011; Kopacz et al., 2011).

In this region of the Himalaya the majority of precipitation occurs during the summer monsoon season, whereas the winter–spring is drier. Summer monsoonal precipitation results in the wet deposition of BC and dust from the atmosphere during transport from emission sources to the study site, and thus lower atmospheric particle concentrations in the Himalaya during summer. The higher summer monsoonal precipitation rate relative to winter also acts to dilute the concentration of impurities distributed across the snow column. Thus, lower atmospheric concentrations and higher snow accumulation keep impurity concentrations lower in summer snow and ice layers.

During the drier winter–spring months the residence time of BC and other aerosols is longer, and observed atmospheric concentrations are higher, particularly during the spring pre-monsoon season. This is the case at NCO-P, where the higher pre-monsoon atmospheric concentrations are attributed to higher vertical mixing layer heights and strong daytime up-valley winds that transport pollutants from low elevation regions (Bonasoni et al., 2010). If atmospheric aerosol concentrations are relatively higher at the study site during the winter–spring, higher deposition of impurities on the glacier surface via dry deposition would occur at this time. Furthermore, because there is less wet removal that occurs during transport from emission sources during the drier winter–spring, there may be greater wet deposition of BC and dust at the study site when localized precipitation does occur. However, there are no atmospheric observations at elevations higher than NCO-P in the region, thus it is not known if the pre-monsoon vertically mixed layer extends to altitudes as high as the study area.

<a href="#">Title Page</a>	
<a href="#">Abstract</a>	<a href="#">Introduction</a>
<a href="#">Conclusions</a>	<a href="#">References</a>
<a href="#">Tables</a>	<a href="#">Figures</a>
<a href="#">◀</a>	<a href="#">▶</a>
<a href="#">◀</a>	<a href="#">▶</a>
<a href="#">Back</a>	<a href="#">Close</a>
<a href="#">Full Screen / Esc</a>	
<a href="#">Printer-friendly Version</a>	
<a href="#">Interactive Discussion</a>	

Based on the above information, we conclude that the higher concentration layers observed in the crevasse profiles are from BC and dust deposited and melt-concentrated during the winter–spring, whereas the thicker but lower concentration layers are from snowfall during the summer monsoon. This is supported by  $M_{BC}$  from the snowpits sampled during November 2009, which are representative of snowfall from the summer monsoon season.  $M_{BC}$  from the monsoon snowfall at all three sites was  $\leq 1 \mu\text{g L}^{-1}$ , consistent with the thicker low  $M_{BC}$  layers observed in the crevasse profiles.

### 3.2 Elevational variations of BC

$M_{BC}$  from the snowpit and crevasse profiles collected during spring 2009 are lower at the high elevation site, and increase with decreasing elevation (Table 1, Fig. 3). The difference in  $M_{BC}$  with elevation is apparent in the background, average and maximum values. This elevation gradient is likely due to greater BC deposition at lower elevations because of higher atmospheric concentrations in the troposphere and/or post-depositional processes leading to enrichment of impurities.

$M_{BC}$  in fresh snowfall sampled at NCO-P (5079 m a.s.l.) in the Khumbu Valley during winter–spring 2009 ranged between  $3\text{--}23 \mu\text{g L}^{-1}$ . This is considerably lower than  $M_{BC}$  in the impurity layers in the crevasse profiles, suggesting that the impurities observed in the crevasse profiles result from dry deposition, and/or post-depositional processes. Snowmelt and concentration of impurities are driven by energy absorption of the impurities in snow (referred to as the “direct effect”), and enhanced absorption by larger snow grain size due to accelerated grain growth from the direct effect (referred to as the 1st indirect effect) (Painter et al., 2007). These effects cause snow metamorphism that can cause impurities in the snowpack to coalesce into a single layer, as observed in annual layers in the crevasse profiles. The coalescence of impurities into a single layer is likely greater at lower elevations due to greater energy fluxes and greater direct and 1st indirect effects of BC. Previous studies have documented concentration of impurities at the glacier surface due to mechanical trapping during conditions of melt or sublimation, with conditions of strong melt resulting in flushing of particles to deeper

<a href="#">Title Page</a>	
<a href="#">Abstract</a>	<a href="#">Introduction</a>
<a href="#">Conclusions</a>	<a href="#">References</a>
<a href="#">Tables</a>	<a href="#">Figures</a>
<a href="#">◀</a>	<a href="#">▶</a>
<a href="#">◀</a>	<a href="#">▶</a>
<a href="#">Back</a>	<a href="#">Close</a>
<a href="#">Full Screen / Esc</a>	
<a href="#">Printer-friendly Version</a>	
<a href="#">Interactive Discussion</a>	



in the snowpack (Xu et al., 2012; Conway et al., 1996). These processes likely occur during the winter–spring, and lessen during the summer monsoon season when impurity concentrations are low, accumulation is higher, and the snow direct and 1st indirect effects are minimized, despite greater incoming solar radiation.

5 The visible wavelengths albedo of Mera glacier was visibly lower than that of clean snow, particularly in the lower elevation areas of the glacier, as seen in a photograph of Mera glacier taken in April 2009 (Fig. 2b). The albedo appears much lower at low elevations (5400 m a.s.l.) relative to the summit of Mera Peak (6400 m). While smaller snow grain size at higher elevations accounts for albedo differences, impurities have  
10 a markedly greater potential to decrease albedo in the visible wavelengths (Warren and Wiscombe, 1980; Flanner et al., 2007).

### 3.3 Albedo and radiative forcing implications

Light absorbing impurities in snow and ice can reduce the surface albedo (largely in the visible wavelengths, but out to 1.1  $\mu\text{m}$ ), interacting with more than half of the at-surface  
15 irradiance (the direct effect) (Painter, 2011; Singh et al., 2010; Painter et al., 2012). This reduction in albedo heats the snowpack by conducting energy from the heated impurities to snow grains, in turn accelerating snow metamorphism, which leads to coarser grains and further reduces snow albedo (the 1st feedback). These forcings warm the snow earlier and lead to an earlier and more rapid melt. The earlier emergence of  
20 glacial ice then markedly increases net energy fluxes and ablation.

Factors that affect the BC-induced albedo reduction include snow grain size, solar zenith angle, snow depth, BC concentration, the BC ice/mixing state, BC particle morphology, and the presence of other absorbing impurities and liquid water (Wiscombe and Warren, 1980; Warren and Wiscombe, 1985; Hansen and Nazarenko, 2004). Previous model, laboratory and observational studies have estimated the albedo reduction due to BC (Warren and Wiscombe, 1980, 1985; Grenfell et al., 1981, 1994; Hadley and Kirchstetter, 2012; Jacobson, 2004; Brandt et al., 2011; Flanner et al., 2007). Albedo reduction by impurities is greater for old snow relative to new snow, and for internally  
25

[Title Page](#)

[Abstract](#)

[Introduction](#)

[Conclusions](#)

[References](#)

[Tables](#)

[Figures](#)

◀

▶

◀

▶

[Back](#)

[Close](#)

[Full Screen / Esc](#)

[Printer-friendly Version](#)

[Interactive Discussion](#)



mixed BC (BC is located in the ice grain) relative to externally mixed BC (BC is separated from the ice particle) (Warren and Wiscombe, 1985; Hansen and Nazarenko, 2004).

Light absorbing impurities besides BC that can cause albedo reductions include 5 dust and light absorbing carbon (colored organics) from biomass burning, humic-like substances, snow algae and bacteria (Andreae and Gelencser, 2006; Takeuchi, 2002; Painter et al., 2007). Albedo reductions from BC will be less in the presence of other 10 light absorbing impurities because the other impurities capture some of the solar radiation that the BC would receive in the absence of other impurities (Kaspari et al., 2011). This is particularly relevant for glaciers in this region where the presence of other impurities can be high.

Because we did not measure spectral albedo at the sample sites, we must infer 15 spectral albedo and light absorbing impurity radiative forcing in snow from modeling constrained by the in situ measurements of <sub>M</sub>BC and dust concentrations. The dust concentrations are inferred from the gravimetric mass rather than the Fe concentrations, since absorption due to Fe is highly dependent on the mineralogy of the dust, which has not been characterized. Here we treat the gravimetrically determined total 20 impurity load as dust, although a portion of the dry mass may also consist of organic material. The near-surface concentrated layer with  $258 \mu\text{g L}^{-1}$  <sub>M</sub>BC and  $9.3 \text{ g L}^{-1}$  dust highlights the potential instantaneous radiative forcings due to <sub>M</sub>BC and dust at Mera La. The maximum concentrations of <sub>M</sub>BC ( $3535 \mu\text{g L}^{-1}$ ) and gravimetric dust ( $28.7 \text{ g L}^{-1}$  dust) were sampled at 154 cm depth. However, we do not estimate the spectral albedo for this layer since it may represent convergence of multiple years of impurities.

We estimated the spectral albedo using the Snow, Ice, and Aerosol Radiative 25 (SNICAR) model (Flanner and Zender, 2006), constrained by the near-surface <sub>M</sub>BC and dust concentrations and using a solar zenith angle of  $5^\circ$  at solar noon. In order to span the range of forcings with varying grain sizes, we use snow optical grain radii of 350 and 750  $\mu\text{m}$ . This span of grain sizes has been found in the presence of heavy impurity concentration loading in the Colorado River Basin (Painter et al., 2013). The

<a href="#">Title Page</a>	
<a href="#">Abstract</a>	<a href="#">Introduction</a>
<a href="#">Conclusions</a>	<a href="#">References</a>
<a href="#">Tables</a>	<a href="#">Figures</a>
<a href="#">◀</a>	<a href="#">▶</a>
<a href="#">◀</a>	<a href="#">▶</a>
<a href="#">Back</a>	<a href="#">Close</a>
<a href="#">Full Screen / Esc</a>	
<a href="#">Printer-friendly Version</a>	
<a href="#">Interactive Discussion</a>	



smaller grain sizes are coincident with the highest concentrations when snowmelt percolation causes grains to grow at depths several cm into the pack, leaving smaller grain sizes at the surface to be detected by remote sensing. The mass absorption coefficient (MAC) of BC is not exactly known, so we also span the range of MAC from  $5.9 \text{ m}^2 \text{ g}^{-1}$  to  $7.5 \text{ m}^2 \text{ g}^{-1}$ . The BC MAC of  $5.9 \text{ m}^2 \text{ g}^{-1}$  is based on the theoretical MAC values calculated from Mie scattering theory for 460 nm light and BC with an index of refraction of ( $n = (2.26, -1.26)$ ) (Schwarz et al., 2013) and the measured mass size distribution of BC volume-equivalent particle diameters (80–500 nm) from snow samples measured at Mera La, whereas the BC MAC of  $7.5 \text{ m}^2 \text{ g}^{-1}$  is based on values reported in the literature (Bond and Bergstrom, 2006; Chang and Charalampopoulos, 1990).

We estimate the clear-sky spectral irradiance for wavelength range 0.305 to 4.995  $\mu\text{m}$  at 0.010  $\mu\text{m}$  intervals on 1 June 2009 for 5400 m elevation at solar noon using the Santa Barbara DISORT Atmospheric Radiative Transfer model (SBDART) (Ricchiazzi et al., 1998). The spectral ratios of reflected flux and irradiance give the spectral albedo and the integral of these albedos weighted by the spectral irradiance spectrum and divided by the sum of irradiance across the spectrum gives the broadband albedo:

$$\alpha = \frac{\sum_{\lambda=0.305 \mu\text{m}}^{4.995 \mu\text{m}} E(\lambda; \theta_0) \cdot \alpha_{\text{sfc}}^{\text{laisi}}(r; \lambda) \Delta \lambda}{\sum_{\lambda=0.305 \mu\text{m}}^{4.995 \mu\text{m}} E(\lambda; \theta_0) \Delta \lambda} \quad (1)$$

where  $\alpha_{\text{sfc}}^{\text{laisi}}$  is the modeled snow spectral albedo with BC and/or dust,  $E$  is the spectral irradiance,  $r$  is the snow optical grain size,  $\lambda$  is wavelength ( $\mu\text{m}$ ), and  $\theta_0$  is the solar zenith angle for irradiance, in this case  $5^\circ$  at solar noon.

The convolution of the differences in spectral albedo from the clean snow spectrum with the spectral irradiance gives an estimate of the direct radiative forcing by the light

## Variations of black carbon and dust in snow and ice

S. Kaspari et al.

[Title Page](#)

[Abstract](#)

[Introduction](#)

[Conclusions](#)

[References](#)

[Tables](#)

[Figures](#)

[◀](#)

[▶](#)

[Back](#)

[Close](#)

[Full Screen / Esc](#)

[Printer-friendly Version](#)

[Interactive Discussion](#)



absorbing impurities (Painter et al., 2013).

$$RF = \sum_{\lambda=0.305\mu\text{m}}^{4.995\mu\text{m}} E(\theta_0; \lambda) \cdot (\alpha_{\text{sfc}}^{\text{clean}}(\lambda; r) - \alpha_{\text{sfc}}^{\text{laisi}}(\lambda; r)) \Delta\lambda \quad (2)$$

where  $\alpha_{\text{sfc}}^{\text{clean}}$  is the modeled clean snow spectral albedo.

5 Clean snow albedos for the 350 and 750  $\mu\text{m}$  grain radii particles for this solar zenith angle are 0.72 and 0.67, respectively (Fig. 3). If BC was the only impurity in the snowpack, the broadband albedos would be 0.65–0.66 and 0.57–0.59, respectively, with associated instantaneous radiative forcings of 75–87  $\text{W m}^{-2}$  and 104–120  $\text{W m}^{-2}$ . These forcings are based on  ${}_{\text{M}}\text{BC}$ , so actual albedo reductions and radiative forcings may  
10 be larger. However, dust was mixed in much larger concentrations with the BC. If dust was the only impurity in the snowpack, the broadband albedos for the 350 and 750  $\mu\text{m}$  snow grain radii would be 0.32 and 0.25, respectively, with associated instantaneous radiative forcings of 488 and 525  $\text{W m}^{-2}$ . If BC and dust are mixed, the albedos are slightly changed from those for the large dust concentrations (< 0.01) and the radiative  
15 forcings only increase by 2–3  $\text{W m}^{-2}$  over those for dust-only.

The optical properties of the BC and dust come from general libraries and not this specific region, and therefore the modeling of radiative forcings are relatively uncertain. Additionally, the proportion of dust that originates from natural as opposed to anthropogenic sources is also not well known, although ice core records indicate that dust  
20 deposition has increased in this region (Thompson et al., 2000; Kaspari et al., 2009). Nevertheless, these results give us a preliminary idea of the order of magnitude and range of uncertainty of maximum forcing by impurities at the lower elevation Mera La site. For this near surface layer, the instantaneous radiative forcings reasonably range from the BC forcings of 75 to 120  $\text{W m}^{-2}$  to the bulk dust only and BC+dust radiative  
25 forcings of 488–525  $\text{W m}^{-2}$ .

While these represent the maximum forcing before the onset of the monsoon, we do not have the time resolution by which to know how impurities accumulated through this

## Variations of black carbon and dust in snow and ice

S. Kaspari et al.

[Title Page](#)

[Abstract](#)

[Introduction](#)

[Conclusions](#)

[References](#)

[Tables](#)

[Figures](#)

◀

▶

[Back](#)

[Close](#)

[Full Screen / Esc](#)

[Printer-friendly Version](#)

[Interactive Discussion](#)



5 melt season and how radiative forcing progressed. Ultimately, airborne and spaceborne imaging spectrometers and field-based spectrometry and in situ measurements will characterize the time variation of radiative forcing. New methods are needed to infer spectral complex refractive indices from bulk samples and to partition them into BC, dust, and organics.

### 3.4 Implications for Himalayan Glaciers, snowmelt and radiative forcing

Glaciers in the eastern Himalaya are summer accumulation type glaciers. During summer, substantial precipitation falls associated with the South Asian monsoon, and ablation is also at a maximum (Ageta and Higuchi, 1984). If the high impurity layers that 10 form during the winter–spring are covered by fresh snowfall during the summer season, the effect of BC and dust on summer glacier melt would be largely eliminated. Conversely, if the impurities are exposed at the glacier surface during the melt season, glacier melt would be accelerated. This could occur if melt results in the re-exposure of impurities at the glacier surface, and/or the melt season is expanded due to a warming 15 climate (Fujita et al., 2007; Yasunari et al., 2010). The spatial distribution of precipitation in this region is largely unknown. However, remote sensing of the Himalaya suggests that for elevations  $< 7000$  m, snow covered area does not increase during summer (Maskey et al., 2011) and therefore these impurities should remain exposed, whereas 20 at higher elevations summer snowfall would diminish the impacts of winter/spring accumulation of BC and dust.

While this study documents substantial BC and dust at 5400 m to result in a reduction of the glacier albedo, it is not clear if sufficient light absorbing impurities are present at higher elevations for a notable reduction in albedo to occur. The maximum  $M_{BC}$  in the snowpits sampled at Mera Col at 6400 m a.s.l. was  $8.4 \mu\text{g L}^{-1}$ .  $M_{BC}$  concentrations in an 25 ice core collected from the col of the nearby East Rongbuk glacier (6518 m a.s.l.) on the northeast side of Mt. Everest and analyzed for BC by the same methods employed in this study also generally had lower  $M_{BC}$  concentrations than the lower elevation sites (Table 1; Kaspari et al., 2011). Relatively low  $M_{BC}$  concentrations on East Rongbuk

[Title Page](#)

[Abstract](#)

[Introduction](#)

[Conclusions](#)

[References](#)

[Tables](#)

[Figures](#)

◀

▶

◀

▶

[Back](#)

[Close](#)

[Full Screen / Esc](#)

[Printer-friendly Version](#)

[Interactive Discussion](#)



and Mera glaciers at  $\sim 6500$  m suggests that, at least over short distances, a strong gradient in BC deposition does not exist between the southern and northern slope of the Himalaya. As stated before,  $M_{BC}$  reported herein represent lower limit BC values, so our results are not conclusive regarding the contribution of BC to albedo reduction on glaciers and seasonal snow at elevations greater than 6000 m a.s.l.. Our results do, however, suggest that BC contributes to a greater albedo reduction at elevations below  $\sim 6000$  m a.s.l., but when in the presence of large dust concentrations, BC contributes little forcing.

To assess potential impacts of BC and dust on snow and ice, variations in the amount of snow and ice with elevation needs to be considered. In the Nepal Himalaya at elevations greater than 6000 m the fraction of land that is snow covered is in excess of 60 % throughout the year, whereas for elevations lower than 6000 m with the exception of February–March it is less than 40 % (Maskey et al., 2011). In the regions with the greatest fraction of snow-covered land BC and dust concentrations are relatively low. However, for land area above 3000 m in the Nepal Himalaya the fraction of land at elevations greater than 6000 m is less than 1 %, whereas 90 % of the land lies in the elevation zone between 4000 and 6000 m (Maskey et al., 2011). Thus, the largest areal extent of snow-covered area lies in the 4000 to 6000 m zone, where BC and dust concentrations in snow and ice were observed to be highest.

That BC and dust-induced albedo reduction and the concentrations of snow and ice varies with elevation has implications for glacial mass balance, water resources and radiative forcing. At elevations above  $\sim 6000$  m lie the accumulation zones of glaciers in this region, and a large fraction of the land area is snow covered. However, the small fraction of land at elevations greater than 6000 m combined with minimal surface melt and relatively low BC and dust concentrations suggest that light absorbing impurities in the high Himalaya does not affect water resources and radiative forcing to the degree that is likely at lower elevations. While our results are described in a binary fashion due to the sampling logistics, the impact of BC and dust on glacier melt and water resources occurs in a continuous convolution of near-surface concentrations, spatial

5

10

15

20

25

Variations of black carbon and dust in snow and ice

S. Kaspari et al.

[Title Page](#)

[Abstract](#)

[Introduction](#)

[Conclusions](#)

[References](#)

[Tables](#)

[Figures](#)

◀

▶

◀

▶

[Back](#)

[Close](#)

[Full Screen / Esc](#)

[Printer-friendly Version](#)

[Interactive Discussion](#)



extent, snow water equivalent, and energy fluxes. At the higher elevations, concentrations are lower, area is smaller, and energy fluxes are smaller in composite, while snow water equivalent (SWE) is relatively high. Nevertheless, BC and dust anomalies (however small) increase net solar radiation and warm the snowpack. At lower snow-covered elevations, concentrations are higher, spatial extent is larger, and energy fluxes are generally larger. The greatest impact on glacier melt comes from the rising of the equilibrium line altitude (ELA) from earlier removal of snow cover, and glacier ice then being subject to markedly greater energy fluxes.

BC and dust have the potential to accelerate glacial and seasonal snowmelt, which could impact water resources if the timing and magnitude of runoff is altered. Using a numerical model applied to BC observed on a Tibetan glacier, Yasunari et al. (2010) estimated that a 2.0–5.2 % albedo reduction from BC deposition could result in a 11.6–33.9 % increase in annual discharge if the reduced albedo snow layer remained at the glacier surface. While this increase in discharge likely overestimates actual increases in discharge since snow with a lower BC concentration and higher albedo is deposited during the summer monsoon, it nevertheless highlights that BC has the potential to accelerate snow/ice melt. However, our findings suggest that in the presence of high dust concentrations, the efficacy of BC to induce melt is lessened. Thus, further research is needed to partition light absorbing impurities into their various components (BC, dust, organics), along with a more holistic treatment of light absorbing impurity induced melt. This is particularly important in the context of determining the degree to which snow and glacier melt is being driven by increased deposition of light absorbing impurities from anthropogenic activities. Since a substantial portion of dust originates from natural sources, partitioning the contribution of BC and dust deposition from anthropogenic as opposed to natural sources is challenging.

<a href="#">Title Page</a>	
<a href="#">Abstract</a>	<a href="#">Introduction</a>
<a href="#">Conclusions</a>	<a href="#">References</a>
<a href="#">Tables</a>	<a href="#">Figures</a>
<a href="#">◀</a>	<a href="#">▶</a>
<a href="#">◀</a>	<a href="#">▶</a>
<a href="#">Back</a>	<a href="#">Close</a>
<a href="#">Full Screen / Esc</a>	
<a href="#">Printer-friendly Version</a>	
<a href="#">Interactive Discussion</a>	

## 4 Conclusions

This study documents seasonal and elevational variations in BC and dust concentrations measured in snow and ice on Mera glacier in the Solu-Khumbu region of Nepal. BC and dust concentrations peak during the winter–spring, and are substantially higher at elevations  $< 6000$  m than  $> 6000$  m due to post-depositional processes including melt and sublimation, and likely greater deposition at lower elevations. Because the largest areal extent of snow and ice resides at elevations  $< 6000$  m, the higher BC and dust concentrations at these elevations can reduce the snow and glacier albedo over large areas, accelerating melt, affecting glacier mass-balance and water resources, and contributing to a positive climate forcing. Radiative transfer modeling constrained by measurements indicates that while BC contributes to accelerated snow and ice melt, the impact of BC is diminished in the presence of dust. However, the time span of the BC exposure at the snow surface in the dry winter–spring season is likely a persistent forcing before impurity convergence, but is not addressed by these single measurements. During the summer, lower BC and dust deposition from summer monsoonal snowfall that coincides with the peak ablation season likely reduces the efficacy of light absorbing impurities to accelerate summer melt.

While this study highlights the effect that BC and dust may be having on Himalayan glaciers, water resources, and climate, it neglects several other important factors. As mentioned before, other light absorbing impurities including colored organics, humic-like substances, and snow algae and bacteria can also contribute to albedo reduction (Andreae and Gelencser, 2006; Painter et al., 2007; Takeuchi, 2002). Further observational studies are needed to assess the relative contribution of different absorbing impurities to albedo reductions and snow and ice melt, including the temporal evolution of how impurities accumulate and radiative forcing progresses through the melt season. Other factors that also contribute to changes in the cryosphere in the Himalaya include higher air temperatures (Yang et al., 2011), changes in snow accumulation (Kaspari et al., 2008), and variations in glacier velocities (Quincey et al., 2009).

## Variations of black carbon and dust in snow and ice

S. Kaspari et al.

[Title Page](#)

[Abstract](#)

[Introduction](#)

[Conclusions](#)

[References](#)

[Tables](#)

[Figures](#)

◀

▶

◀

▶

[Back](#)

[Close](#)

[Full Screen / Esc](#)

[Printer-friendly Version](#)

[Interactive Discussion](#)



**Acknowledgements.** We thank Tshering Dorgi Sherpa, Jesse Cunningham and the Nepali staff for assistance in the field during the spring 2009 field season, Yves Arnaud and Patrick Wagnon for collecting the fall 2009 snow samples and for valuable information about the Mera region, and EV-K2-CNR for collection of fresh snow samples at NCO-P and assistance with permitting.

5 S. McKenzie Skiles assisted with radiative transfer simulations, and Walter Szeliga calculated the MAC value based on measured BC size distributions. This research was funded by the National Science Foundation (OISE-0653933 and EAR-0957935), NASA project NNX10AO97G, and partially supported by the Office of the Dean, College of the Sciences, Central Washington University, Ellensburg, Washington. Collection of fresh snow samples at NCO-P was carried

10 out within the framework of the EV-K2-CNR Project in collaboration with the Nepal Academy of Science and Technology as foreseen by the Memorandum of Understanding between Nepal and Italy, and thanks to contributions from the Italian National Research Council. MG received financial support from the Swiss National Science Foundation.

## References

15 Ageta, Y. and Higuchi, K.: Estimation of mass balance components of a summer-accumulation type glacier in the Nepal Himalaya, *Geogr. Ann.*, 66, 249–255, 1984.

Andreae, M. O. and Gelencsér, A.: Black carbon or brown carbon? The nature of light-absorbing carbonaceous aerosols, *Atmos. Chem. Phys.*, 6, 3131–3148, doi:10.5194/acp-6-3131-2006, 2006.

20 Barnett, T. P., Adam, J. C., and Lettenmaier, D. P.: Potential impacts of a warming climate on water availability in snow-dominated regions, *Nature*, 438, 303–309, doi:10.1038/nature04141, 2005.

Bonasoni, P., Laj, P., Marinoni, A., Sprenger, M., Angelini, F., Arduini, J., Bonafè, U., Calzolari, F., Colombo, T., Decesari, S., Di Biagio, C., di Sarra, A. G., Evangelisti, F., Duchi, R., Facchini, M.C., Fuzzi, S., Gobbi, G. P., Maione, M., Panday, A., Roccato, F., Sellegrini, K., Venzac, H., Verza, G.P., Villani, P., Vuillermoz, E., and Cristofanelli, P.: Atmospheric Brown Clouds in the Himalayas: first two years of continuous observations at the Nepal Climate Observatory-Pyramid (5079 m), *Atmos. Chem. Phys.*, 10, 7515–7531, doi:10.5194/acp-10-7515-2010, 2010.

<a href="#">Title Page</a>	
<a href="#">Abstract</a>	<a href="#">Introduction</a>
<a href="#">Conclusions</a>	<a href="#">References</a>
<a href="#">Tables</a>	<a href="#">Figures</a>
<a href="#">◀</a>	<a href="#">▶</a>
<a href="#">◀</a>	<a href="#">▶</a>
<a href="#">Back</a>	<a href="#">Close</a>
<a href="#">Full Screen / Esc</a>	
<a href="#">Printer-friendly Version</a>	
<a href="#">Interactive Discussion</a>	



Bond, T. and Bergstrom, R.: Light absorption by carbonaceous particles: an investigative review, *Aerosol Sci. Tech.*, 40, 27–67, 2006.

Bond, T., Bhardwaj, E., Dong, R., Jogani, R., Jung, S., Roden, C., Streets, D. G., and Trautmann, N.: Historical emissions of black and organic carbon aerosol from energy-related combustion, 1850–2000, *Global Biogeochem. Cy.*, 21, GB2018, doi:10.1029/2006GB002840, 2007.

Bond, T. C., Streets, D. G., Yarber, K. F., Nelson, S. M., Woo, J. H., and Klimont, Z.: A technology-based global inventory of black and organic carbon emissions from combustion, *J. Geophys. Res.-Atmos.*, 109, D14203, doi:10.1029/2003JD003697, 2004.

Bond, T., Doherty, S., Fahey, D. W., Forster, P. M., Berntsen, T., DeAngelo, B. J., Flanner, M. G., Ghan, S., Kärcher, B., Koch, D., Kinne, S., Kondo, Y., Quinn, P. K., Sarofim, M. C., Schultz, M. G., Schulz, M., Venkataraman, C., Zhang, H., Zhang, S., Bellouin, N., Guttikunda, S. K., Hopke, P. K., Jacobson, M. Z., Kaiser, J. W., Klimont, Z., Lohmann, U., Schwarz, J. P., Shindell, D., Storelvmo, T., Warren, S. G., and Zender, C. S.: Bounding the role of black carbon in the climate system: a scientific assessment, *J. Geophys. Res.-Atmos.*, 118, 5380–5552, doi:10.1002/jgrd.50171, 2013.

Brandt, R. E., Warren, S. G., and Clarke, A. D.: A controlled snowmaking experiment testing the relation between black carbon content and reduction of snow albedo, *J. Geophys. Res.-Atmos.*, 116, D08109, doi:10.1029/2010jd015330, 2011.

Chang, H. and Charalampopoulos, T. T.: Determination of the wavelength dependence of refractive indices of flame soot, in: *Proceedings: Mathematical and Physical Sciences, Proc. R. Soc. Lond. A*, 430, 577–591, doi:10.1098/rspa.1990.0107, 1990.

Cong, Z., Kang, S., and Qin, D.: Seasonal features of aerosol particles recorded in snow from Mt. Qomolangma (Everest) and their environmental implications, *J. Environ. Sci.*, 21, 914–919, 2009.

Conway, H., Gades, A., and Raymond, C. F.: Albedo of dirty snow during conditions of melt, *Water Resour. Res.*, 32, 1713–1718, 1996.

Flanner, M. G. and Zender, C. S.: Linking snowpack microphysics and albedo evolution, *J. Geophys. Res.-Atmos.*, 111, D12208, doi:10.1029/2005jd006834, 2006.

Flanner, M. G., Zender, C. S., Randerson, J. T., and Rasch, P. J.: Present-day climate forcing and response from black carbon in snow, *J. Geophys. Res.*, 112, doi:10.1029/2006JD008003, 2007.

**Variations of black carbon and dust in snow and ice**

S. Kaspari et al.

[Title Page](#)[Abstract](#)[Introduction](#)[Conclusions](#)[References](#)[Tables](#)[Figures](#)[◀](#)[▶](#)[◀](#)[▶](#)[Back](#)[Close](#)[Full Screen / Esc](#)[Printer-friendly Version](#)[Interactive Discussion](#)

Flanner, M. G., Zender, C. S., Hess, P. G., Mahowald, N. M., Painter, T. H., Ramanathan, V., and Rasch, P. J.: Springtime warming and reduced snow cover from carbonaceous particles, *Atmos. Chem. Phys.*, 9, 2481–2497, doi:10.5194/acp-9-2481-2009, 2009.

Fujita, K., Ohta, T., and Ageta, Y.: Characteristics and climatic sensitivities of runoff from a cold-type glacier on the Tibetan Plateau, *Hydrol. Process.*, 21, 2882–2891, doi:10.1002/hyp.6505, 2007.

Gautam, R., Hsu, N. C., Lau, W. K. M., and Yasunari, T. J.: Satellite observations of desert dust-induced Himalayan snow darkening, *Geophys. Res. Lett.*, 40, 988–993, doi:10.1002/grl.50226, 2013.

Grenfell, T. C., Perovich, D. K., and Ogren, J. A.: Spectral albedos of an alpine snowpack, *Cold Reg. Sci. Technol.*, 4, 121–127, 1981.

Grenfell, T. C., Warren, S., and Mullen, P. C.: Reflection of solar radiation by the Antarctic snow surface at ultraviolet, visible, and near-infrared wavelengths, *J. Geophys. Res.*, 99, 18669–18684, 1994.

Hadley, O. L. and Kirchstetter, T. W.: Black carbon reduction of snow albedo, *Nature Climate Change*, 2, 437–440, 2012.

Hansen, J. and Nazarenko, L.: Soot climate forcing via snow and ice albedos, *P. Natl. Acad. Sci. USA*, 101, 423–428, 2004.

Immerzeel, W. W., van Beek, L. P. H., and Bierkens, M. F. P.: Climate change will affect the Asian water towers, *Science*, 328, 1382–1385, doi:10.1126/science.1183188, 2010.

Jacobson, M. Z.: Climate response of fossil fuel and biofuel soot, accounting for soot's feedback to snow and sea ice albedo and emissivity, *J. Geophys. Res.*, 109, D21201, doi:10.1029/2004JD004945, 2004.

Kaspari, S., Hooke, R., Mayewski, P. A., Kang, S., Hou, S., and Qin, D.: Snow accumulation rate on Qomolangma (Mt. Everest): synchronicity with sites across the Tibetan Plateau on 50–100 year timescales, *J. Glaciol.*, 54, 343–352, 2008.

Kaspari, S., Mayewski, P. A., Handley, M. J., Kang, S., Hou, S., Maasch, K., and Qin, D.: A high-resolution record of atmospheric dust variability and composition since 1650 AD from a Mt. Everest Ice Core, *J. Climate*, 22, 3910–3925, doi:10.1175/2009JCLI2518.1, 2009.

Kaspari, S., Schwikowski, M., Gysel, M., Flanner, M. G., Kang, S., Hou, S., and Mayewski, P. A.: Recent increase in black carbon concentrations from a Mt. Everest ice core spanning 1860–2000 AD, *Geophys. Res. Lett.*, 38, L04703, doi:10.1029/2010GL046096R, 2011.

Variations of black carbon and dust in snow and ice

S. Kaspari et al.

[Title Page](#)

[Abstract](#)

[Introduction](#)

[Conclusions](#)

[References](#)

[Tables](#)

[Figures](#)

◀

▶

◀

▶

[Back](#)

[Close](#)

[Full Screen / Esc](#)

[Printer-friendly Version](#)

[Interactive Discussion](#)



Kopacz, M., Mauzerall, D. L., Wang, J., Leibensperger, E. M., Henze, D. K., and Singh, K.: Origin and radiative forcing of black carbon transported to the Himalayas and Tibetan Plateau, *Atmos. Chem. Phys.*, 11, 2837–2852, doi:10.5194/acp-11-2837-2011, 2011.

Liu, X., Xu, B., Yao, T., Wang, N., and Wu, G.: Carbonaceous particles in Muztag Ata ice core, 5 West Kunlun Mountains, China, *Chinese Sci. Bull.*, 53, 3379–3386, 2008.

Marinoni, A., Cristofanelli, P., Laj, P., Duchi, R., Calzolari, F., Decesari, S., Sellegri, K., Vuiller-moz, E., Verza, G. P., Villani, P., and Bonasoni, P.: Aerosol mass and black carbon concentrations, a two year record at NCO-P (5079 m, Southern Himalayas), *Atmos. Chem. Phys.*, 10, 8551–8562, doi:10.5194/acp-10-8551-2010, 2010.

Maskey, S., Uhlenbrook, S., and Ojha, S.: An analysis of snow cover changes in the Himalayan region using MODIS snow products and in-situ temperature data, *Climatic Change*, 108, 391–400, doi:10.1007/s10584-011-0181-y, 2011.

Ming, J., Cachier, H., Xiao, C., Qin, D., Kang, S., Hou, S., and Xu, J.: Black carbon record based on a shallow Himalayan ice core and its climatic implications, *Atmos. Chem. Phys.*, 8, 15 1343–1352, doi:10.5194/acp-8-1343-2008, 2008.

Ming, J., Xiao, C., Cachier, H., Qin, D., Qin, X., Li, Z., and Pu, J.: Black carbon (BC) in the snow of glaciers in west China and its potential effects on albedos, *Atmos. Res.*, 92, 114–123, 2009.

Ming, J., Du, Z., Xiao, C., Xu, X., and Zhang, D.: Darkening of the mid-Himalaya glaciers since 2000 and the potential causes, *Environ. Res. Lett.*, 7, 014021, doi:10.1088/1748-20 9326/7/1/014021, 2012.

Painter, T. H.: Comment on Singh and others, “Hyperspectral analysis of snow reflectance to understand the effects of contamination and grain size”, *J. Glaciol.*, 57, 183–185, 2011.

Painter, T., Barrett, A. P., Landry, C. C., Neff, J. C., Cassidy, M. P., Lawrence, C. R., McBride, K. E., and Farmer, G. L.: Impact of disturbed desert soils on duration of mountain snow cover, *Geophys. Res. Lett.*, 34, L12502, doi:10.1029/2007GL030284, 2007.

Painter, T. H., Skiles, S. M., Deems, J. S., Bryant, A. C., and Landry, C. C.: Dust radiative forcing in snow of the upper Colorado River Basin: Part I. A 6-year record of energy balance, radiation, and dust concentrations, *Water Resour. Res.*, 48, W07521, 30 doi:10.1029/2012WR011985, 2012.

Painter, T. H., Seidel, F., Bryant, A. C., Skiles, S. M., and Rittger, K.: Imaging spectroscopy of albedo and radiative forcing by light absorbing impurities in mountain snow, *J. Geophys. Res.-Atmos.*, 118, 9511–9523, doi:10.1002/jgrd.50520, 2013.

**Variations of black carbon and dust in snow and ice****S. Kaspari et al.**[Title Page](#)[Abstract](#)[Introduction](#)[Conclusions](#)[References](#)[Tables](#)[Figures](#)[◀](#)[▶](#)[Back](#)[Close](#)[Full Screen / Esc](#)[Printer-friendly Version](#)[Interactive Discussion](#)

Petzold, A., Ogren, J. A., Fiebig, M., Laj, P., Li, S.-M., Baltensperger, U., Holzer-Popp, T., Kinne, S., Pappalardo, G., Sugimoto, N., Wehrli, C., Wiedensohler, A., and Zhang, X.-Y.: Recommendations for reporting "black carbon" measurements, *Atmos. Chem. Phys.*, 13, 8365–8379, doi:10.5194/acp-13-8365-2013, 2013.

5 Quincey, D. J., Luckman, A., and Benn, D.: Quantification of Everest region glacier velocities between 1992 and 2002, using satellite radar interferometry and feature tracking, *J. Glaciol.*, 55, 596–606, 2009.

Ramanathan, V. and Carmichael, G. R.: Global and regional climate changes due to black carbon, *Nat. Geosci.*, 1, 221–227, 2008.

10 Ricchiazzi, P., Yang, S. R., Gautier, C., and Sowle, D.: SBDART: a research and teaching software tool for plane-parallel radiative transfer in the Earth's atmosphere, *B. Am. Meteorol. Soc.*, 79, 2101–2114, 1998.

Schwarz, J. P., Gao, R. S., Fahey, D. W., Thomson, D. S., Watts, L. A., Wilson, J. C., Reeves, J. M., Darbeheshti, M., Baumgardner, D. G., Kok, G. L., Chung, S. H., Schulz, M., Hendricks, J., Lauer, A., Kärcher, B., Slowik, J. G., Rosenlof, K. H., Thompson, T. L., Langford, A. O., Loewenstein, M., and Aikin, K. C.: Single-particle measurements of midlatitude black carbon and light-scattering aerosols from the boundary layer to the lower stratosphere, *J. Geophys. Res.*, 111, D16207, doi:10.1029/2006JD007076, 2006.

15 Schwarz, J. P., Doherty, S. J., Li, F., Ruggiero, S. T., Tanner, C. E., Perring, A. E., Gao, R. S., and Fahey, D. W.: Assessing Single Particle Soot Photometer and Integrating Sphere/Integrating Sandwich Spectrophotometer measurement techniques for quantifying black carbon concentration in snow, *Atmos. Meas. Tech.*, 5, 2581–2592, doi:10.5194/amt-5-2581-2012, 2012.

Schwarz, J. P., Gao, R. S., Perring, A. E., Spackman, J. R., and Fahey, D. W.: Black carbon aerosol size in snow, *Nat. Sci. Reports*, 3, 1356, doi:10.1038/srep01356, 2013.

20 Singh, S. K., Kulkarni, A., and Chaudhary, B. S.: Hyperspectral analysis of snow reflectance to understand the effects of contamination and grain size, *Ann. Glaciol.*, 51, 83–88, 2010.

Slowik, J. G., Cross, E. S., Han, J., Davidovits, P., Onasch, T. B., Jayne, J. T., Williams, L. R., Canagaratna, M. R., Worsnop, D. R., Chakrabarty, R. K., Moosmüller, H., Arnott, W. P., Schwarz, J. P., Gao, R. S., Fahey, D. W., Kok, G. L., and Petzold, A.: An inter-comparison of instruments measuring black carbon content of soot particles, *Aerosol Sci. Tech.*, 41, 295–314, 2007.

25 Stephens, M., Turner, N., and Sandberg, J.: Particle identification by laser-induced incandescence in a solid-state laser cavity, *Appl. Optics*, 42, 3726–3736, 2003.

[Title Page](#)

[Abstract](#)

[Introduction](#)

[Conclusions](#)

[References](#)

[Tables](#)

[Figures](#)

[◀](#)

[▶](#)

[◀](#)

[▶](#)

[Back](#)

[Close](#)

[Full Screen / Esc](#)

[Printer-friendly Version](#)

[Interactive Discussion](#)



Variations of black carbon and dust in snow and ice

S. Kaspari et al.

[Title Page](#)

[Abstract](#)

[Introduction](#)

[Conclusions](#)

[References](#)

[Tables](#)

[Figures](#)

[|◀](#)

[▶|](#)

[◀](#)

[▶](#)

[Back](#)

[Close](#)

[Full Screen / Esc](#)

[Printer-friendly Version](#)

[Interactive Discussion](#)



Yasunari, T. J., Bonasoni, P., Laj, P., Fujita, K., Vuillermoz, E., Marinoni, A., Cristofanelli, P., Duchi, R., Tartari, G., and Lau, K.-M.: Estimated impact of black carbon deposition during pre-monsoon season from Nepal Climate Observatory – Pyramid data and snow albedo changes over Himalayan glaciers, *Atmos. Chem. Phys.*, 10, 6603–6615, doi:10.5194/acp-10-6603-2010, 2010.

5

ACPD

13, 33491–33521, 2013

Discussion Paper | Discussion Paper

## Variations of black carbon and dust in snow and ice

S. Kaspari et al.

[Title Page](#)

[Abstract](#)

[Introduction](#)

[Conclusions](#)

[References](#)

[Tables](#)

[Figures](#)

◀

▶

[Back](#)

[Close](#)

[Full Screen / Esc](#)

[Printer-friendly Version](#)

[Interactive Discussion](#)



## Variations of black carbon and dust in snow and ice

S. Kaspari et al.

**Table 1.**  $M_{BC}$  and Fe in snow and ice samples from Mera glacier. \* Values reported for the Everest ice core are based on the high-resolution data spanning 1975–2002 (from Kaspari et al., 2011).

Spring 2009					
	Mera La	Mera High Camp	Mera Col	Everest Ice Core*	
elevation (m)	5400	5800	6400	6518	
$n$	34	18	18	496	
$M_{BC}$ $\mu\text{g L}^{-1}$	max average median	3535.0 180.0 12.1	318.9 24.4 4.9	8.4 1.0 0.2	75.3 1.5 0.5
Fe $\mu\text{g L}^{-1}$	max average median	283 040.0 18 674.8 525.0	27 096.0 1760.1 56.8	2357.2 199.1 9.0	2313.3 104.3 28.8

\* Based on high resolution data 1975–2002, and BC concentrations have been corrected based on Aquadag standards.

- [Title Page](#)
- [Abstract](#) | [Introduction](#)
- [Conclusions](#) | [References](#)
- [Tables](#) | [Figures](#)
- [◀](#) | [▶](#)
- [◀](#) | [▶](#)
- [Back](#) | [Close](#)
- [Full Screen / Esc](#)
- [Printer-friendly Version](#)
- [Interactive Discussion](#)



**Variations of black carbon and dust in snow and ice**

S. Kaspari et al.

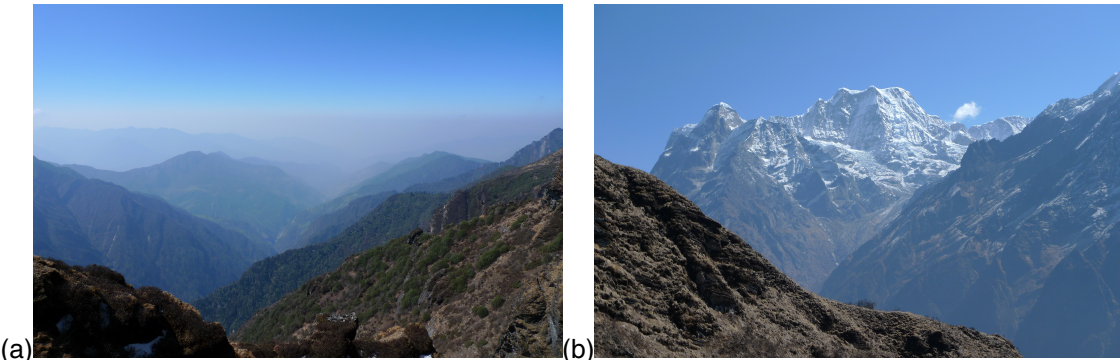


**Fig. 1.** Photographs taken from the same location in the Inkhu Khola Valley, Solu-Khumbu, Nepal at  $\sim 4300$  m. Picture (a) looks south. Note the presence of the Atmospheric Brown Cloud (a combination of BC, other pollutants and dust). Picture (b) looks northwards towards the crest of the Himalaya (here seeing the south side of Mera peak).

<a href="#">Title Page</a>	<a href="#">Abstract</a>	<a href="#">Introduction</a>
<a href="#">Conclusions</a>	<a href="#">References</a>	
<a href="#">Tables</a>	<a href="#">Figures</a>	
<a href="#">◀</a>	<a href="#">▶</a>	
<a href="#">◀</a>	<a href="#">▶</a>	
<a href="#">Back</a>	<a href="#">Close</a>	
<a href="#">Full Screen / Esc</a>		
<a href="#">Printer-friendly Version</a>		
<a href="#">Interactive Discussion</a>		



## Variations of black carbon and dust in snow and ice

S. Kaspari et al.

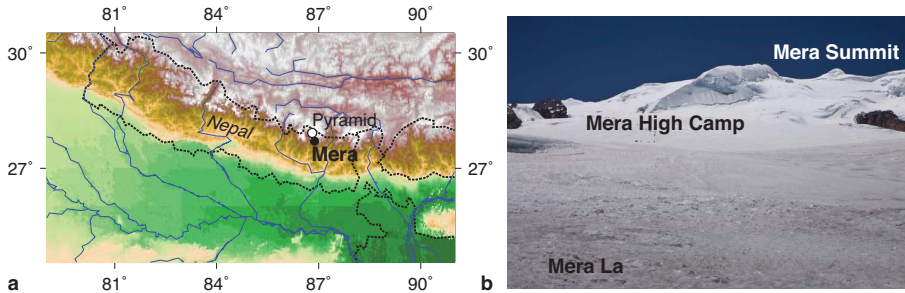


**Fig. 2.** (a) Location of Mera Peak and Pyramid Observatory, and (b) Picture of Mera Glacier taken during April 2009 showing the location of Mera La (5400 m a.s.l.), Mera High Camp (5800 m a.s.l.), and Mera Summit (6400 m a.s.l.). Photo taken by Jesse Cunningham.

<a href="#">Title Page</a>	
<a href="#">Abstract</a>	<a href="#">Introduction</a>
<a href="#">Conclusions</a>	<a href="#">References</a>
<a href="#">Tables</a>	<a href="#">Figures</a>

<a href="#">◀</a>	
<a href="#">◀</a>	<a href="#">▶</a>
<a href="#">Back</a>	
<a href="#">Close</a>	

<a href="#">Full Screen / Esc</a>	
<a href="#">Printer-friendly Version</a>	<a href="#">Interactive Discussion</a>

## Variations of black carbon and dust in snow and ice

S. Kaspari et al.

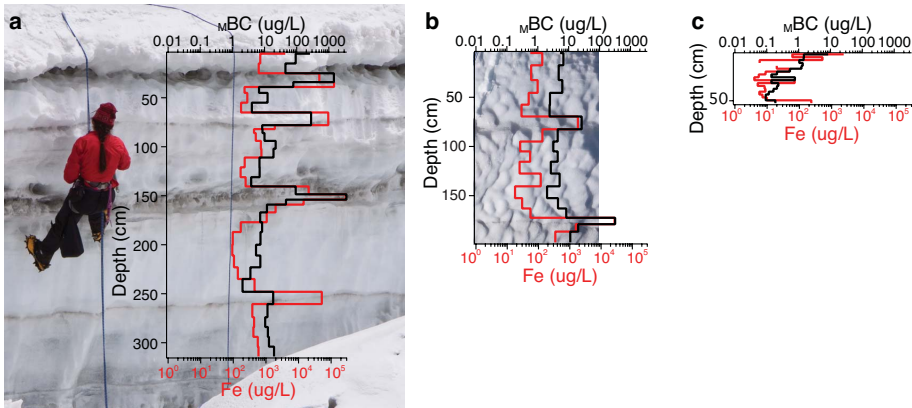


**Fig. 3.**  $mBC$  and Fe (used as a dust proxy) concentrations from Mera glacier crevasses profiles and snowpits from (a) Mera La (5400 m a.s.l.), (b) below Mera High Camp (5800 m a.s.l.), and (c) from a snowpit near the summit of Mera Peak (6400 m a.s.l.).

[Title Page](#)[Abstract](#)[Introduction](#)[Conclusions](#)[References](#)[Tables](#)[Figures](#)[|◀](#)[▶|](#)[Back](#)[Close](#)[Full Screen / Esc](#)[Printer-friendly Version](#)[Interactive Discussion](#)

## Variations of black carbon and dust in snow and ice

S. Kaspari et al.

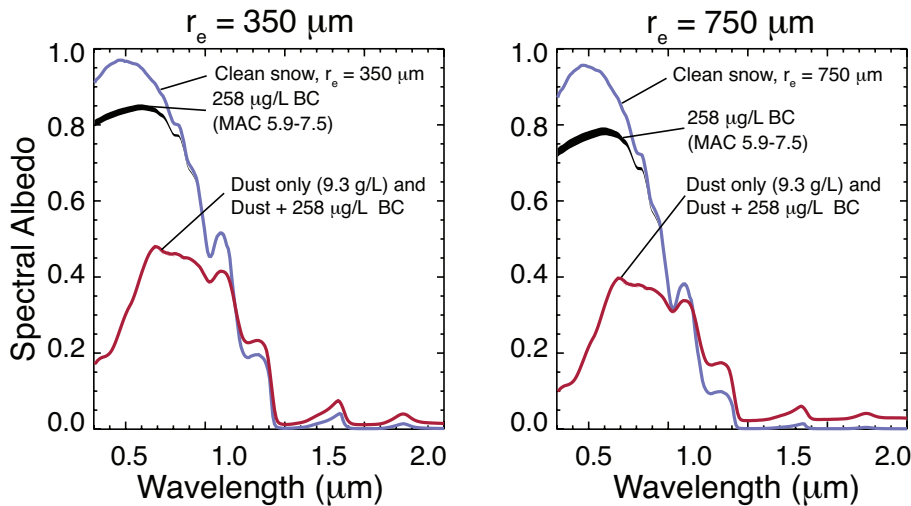


**Fig. 4.** Modeled spectral albedos for the near surface layer at Mera La based on  $_{\text{M}}\text{BC} = 258 \mu\text{g L}^{-1}$  and dust =  $9.3 \text{ g L}^{-1}$  assuming snow optical grain radius of **(a)**  $350 \mu\text{m}$  and **(b)**  $750 \mu\text{m}$ .

- [Title Page](#)
- [Abstract](#) [Introduction](#)
- [Conclusions](#) [References](#)
- [Tables](#) [Figures](#)
- [◀](#) [▶](#)
- [◀](#) [▶](#)
- [Back](#) [Close](#)
- [Full Screen / Esc](#)
- [Printer-friendly Version](#)
- [Interactive Discussion](#)